

## Technicolor with a massless scalar doublet

Christopher D. Carone\* and Howard Georgi†

*Lyman Laboratory of Physics, Harvard University, Cambridge, Massachusetts 02138*

(Received 5 August 1993)

We consider a minimal technicolor model in which the ordinary and technicolor sectors are coupled by a massless scalar doublet. When technicolor interactions become strong, the resulting technicolor condensate not only breaks the electroweak symmetry, but also causes the scalar to develop a vacuum expectation value. With the appropriate choice of the scalar's Yukawa couplings, fermion masses are generated, giving us the conventional pattern of flavor symmetry breaking. Although no explicit scalar mass term appears in the full Lagrangian of the model, the pseudoscalar states that remain in the low-energy effective theory gain sufficient mass through technicolor interactions to evade detection. We show that this model does not generate unacceptably large flavor-changing neutral currents, and is consistent with the experimental constraints on oblique electroweak radiative corrections. We determine the experimentally allowed region of the model's parameter space, and discuss the significance of a phenomenologically viable model that has no arbitrary dimensionful parameters. In terms of parameter counting, our model is the simplest possible extension of the standard model.

PACS number(s): 12.60.Nz

### I. INTRODUCTION

Technicolor models provide an elegant mechanism for electroweak symmetry breaking, but give no natural explanation for the generation of fermion masses. A number of different scenarios have been proposed to solve this problem, including extended technicolor (ETC) models [1], and composite technicolor standard models (CTSM's) [2], but neither of these has been free of other serious shortcomings. ETC models that can accommodate a heavy top quark often can do so only at the expense of generating large flavor-changing neutral current (FCNC) effects. While CTSM's have a Glashow-Iliopoulos-Maiani (GIM) mechanism built into the technicolor sector to minimize this problem, all the realistic examples that have been proposed require many new gauge groups beyond those of the standard model, and therefore these models become aesthetically unappealing. A simple alternative to ETC and CTS models that suffers from neither of these drawbacks is technicolor with a scalar doublet [3]. The scalar communicates electroweak symmetry breaking to the ordinary fermions in a way that does not generate large FCNC effects.

In previous phenomenological studies of technicolor with a single scalar doublet, it was assumed that the scalar had a significant  $SU(2) \times U(1)$  invariant mass, and that quartic terms in the scalar potential could be ignored. The resulting analysis established that the single scalar doublet model was phenomenologically viable over a wide range of the model's parameters. In particular, the model could account for a heavy top quark without generating large flavor-changing neutral currents, and

without exceeding the experimental bounds on the electroweak  $S$  and  $T$  parameters [4]. Part of this success was achieved at the expense of allowing an undetermined dimensionful parameter in the theory, namely, the mass of the scalar doublet,  $M_\phi$ . A simple way to account for this unknown scale is to assume that the scalar is composite, and that its mass is calculable given knowledge of the detailed dynamics of a full, high-energy theory. In this paper, we will explore another alternative, namely, that the scalar is fundamental and that  $M_\phi \equiv 0$ . In this limit, the Lagrangian for our model contains no arbitrary dimensionful parameters. Although the original scalar doublet is now massless, we will see that technicolor interactions are sufficient to give the physical scalar states in the low-energy effective theory masses large enough to ensure that they are not detected. In addition, we will show that FCNC effects are not unacceptably large, and electroweak oblique corrections do not exceed current experimental bounds. In short, the model is again phenomenologically viable. Furthermore, because of the absence of the scalar mass term, the model has only two more parameters than the simplest version of standard model. In this sense, it is the simplest possible extension. In addition, in some allowed regions of the parameter space, the model differs significantly from the more conventional technicolor models discussed in [4].

The paper is organized as follows. In Sec. II, we describe the basic features of the model. In Sec. III, we construct a low-energy effective chiral Lagrangian to describe the physics of the scalar states below the electroweak scale. In Sec. IV, we study the effects of Coleman-Weinberg radiative corrections on the scalar potential. In Sec. V, we set up the analysis of flavor-changing neutral currents in the model. In Sec. VI, we determine the region in the model's parameter space that is excluded by experimental constraints, and discuss possible experimental signatures. In Sec. VII, we discuss the oblique electroweak radiative corrections and present our

\*Electronic address: carone@huhepl.harvard.edu

†Electronic address: georgi@huhepl.harvard.edu

estimate of the low-energy contributions to the  $S$  and  $T$  parameters. In Sec. VIII, we consider the phenomenology of the region of the model's parameter space that is not adequately described by an effective chiral Lagrangian. In the final section we summarize our conclusions.

## II. THE MODEL

The gauge structure of the model is simply the direct product of the technicolor and standard model gauge groups:  $SU(N)_{TC} \times SU(3)_C \times SU(2)_W \times U(1)_Y$ .<sup>1</sup> The technicolor singlet fermions are exactly those of the standard model, in the usual  $SU(2)_W$  representations of left-handed doublets and right-handed singlets:

$$\begin{aligned} L_L &= \begin{bmatrix} l \\ \nu \end{bmatrix}_L, \quad l_R, \\ Q_L &= \begin{bmatrix} U \\ D \end{bmatrix}_L, \quad U_R, \quad D_R. \end{aligned} \quad (2.1)$$

Here  $l \equiv (e, \mu, \tau)$ ,  $\nu \equiv (\nu_e, \nu_\mu, \nu_\tau)$ ,  $U \equiv (u, c, t)$ , and  $D \equiv (d, s, b)$ . We assume that the technicolor sector is minimal; i.e., it consists of two techniflavors  $p$  and  $m$  that also transform under  $SU(2)_W$  as a left-handed doublet and two right-handed singlets:

$$\Upsilon_L = \begin{bmatrix} p \\ m \end{bmatrix}_L, \quad p_R, \quad m_R. \quad (2.2)$$

We assign the hypercharges  $Y(\Upsilon_L)=0$ ,  $Y(p_R)=\frac{1}{2}$ , and  $Y(m_R)=-\frac{1}{2}$  so that the model is free of gauge anomalies. In addition,  $p$  and  $m$  each transform in the fundamental representation of  $SU(N)_{TC}$ .

When technicolor becomes strong at a scale  $\approx 4\pi f$ , the technifermions' chiral symmetries spontaneously break, and the technifermions form a condensate

$$\langle \bar{p}p + \bar{m}m \rangle \approx 4\pi f^3, \quad (2.3)$$

where  $f$  is the technipion decay constant. The condensate breaks the original  $SU(2)_W \times U(1)_Y$  electroweak symmetry down to  $U(1)_{EM}$ , giving mass to the  $W$  and  $Z$  bosons. The ordinary fermions, however, are left unaffected by electroweak symmetry breaking, and will remain massless unless we provide some additional mechanism.

To couple the ordinary fermions to the technicolor condensate, we introduce a massless scalar field  $\phi$ , that transforms as an  $SU(2)_W$  doublet, with hypercharge  $Y(\phi)=\frac{1}{2}$ . The scalar has Yukawa couplings to both the technifermions,

$$\mathcal{L}_{\phi T} = \bar{\Upsilon}_L \tilde{\phi} h_+ p_R + \bar{\Upsilon}_L \phi h_- m_R + \text{H.c.}, \quad (2.4)$$

and to the ordinary fermions,

$$\mathcal{L}_{\phi f} = \bar{L}_L \tilde{\phi} h_l l_R + \bar{Q}_L \tilde{\phi} h_U U_R + \bar{Q}_L \phi h_D D_R + \text{H.c.} \quad (2.5)$$

When the technifermions condense, the scalar develops a vacuum expectation value that generates mass terms for the ordinary fermions. We will see how this works explicitly in Sec. III. The coupling matrices  $h_f$  are proportional to the fermion mass matrices and generate the usual pattern of flavor symmetry breaking of the standard model; in particular, the quarks mix via the conventional Cabibbo-Kobayashi-Maskawa (CKM) matrix.

The new free parameters in our model that are associated with the scalar are the Yukawa couplings ( $h_+, h_-$ ) and the technicolor scale  $\Lambda_{TC}$ . The value of  $\Lambda_{TC}$  will be determined by the  $SU(2) \times U(1)$ -breaking scale (although in a nontrivial way), just as this scale determines the value of the scalar mass term in the simplest standard model. Thus the two "new" parameters can be taken to be  $h_\pm$ . As in the simplest standard model, the physics also depends on the unknown  $(\phi^\dagger \phi)^2/2$  coupling in the scalar potential, which we will call  $\lambda$ . Our aim is to maximally constrain these parameters given the current experimental limits on the relevant physical processes. However, it will be more convenient for us to express our results in terms of the equivalent set of parameters  $\lambda$ ,  $h$ , and  $\delta$ , where

$$h = (h_+ + h_-)/2, \quad \delta = (h_+ - h_-)/(h_+ + h_-). \quad (2.6)$$

In this parametrization, the technicolor sector of the model is custodial isospin conserving when  $\delta=0$ , and maximally isospin violating when  $\delta=1$ . Since custodial isospin violation centers at order  $\delta^2 h^2$  in the chiral expansion, the lowest-order results we present in Sec. III, V, and VI, will depend on  $\lambda$  and  $h$  exclusively. Thus, we will devote much of our effort to identifying the areas of the  $\lambda$ - $h$  plane that are excluded by experiment. The parameter  $\delta$  will be of relevance in Sec. VII where we estimate the nonstandard contributions to the  $T$  parameter. We will show that  $\delta$  can be set to its maximum value throughout much of the allowed region of the  $\lambda$ - $h$  plane, without generating dangerously large corrections to  $T$ . Thus, we will find that it is not necessary to fine-tune  $\delta$  in order to satisfy the experimental constraints.

## III. THE EFFECTIVE CHIRAL LAGRANGIAN

In this section, we construct an effective chiral Lagrangian for our model to describe the physical scalar degrees of freedom below the technicolor scale. This approach is possible because the technicolor kinetic terms have an  $SU(2)_L \times SU(2)_R$  chiral symmetry that is broken spontaneously to a diagonal  $SU(2)_c$ ; the latter is the well-known custodial  $SU(2)$  which prevents the  $T$  parameter from deviating greatly from zero. The pseudo Goldstone bosons that result from the chiral symmetry breaking are the isotriplet of technipions:

$$\Pi = \frac{1}{\sqrt{2}} \begin{bmatrix} \pi^0/\sqrt{2} & \pi^+ \\ \pi^- & -\pi^0/\sqrt{2} \end{bmatrix}. \quad (3.1)$$

The chiral Lagrangian analysis would parallel that of QCD except that the chiral symmetry of interest to us

<sup>1</sup>We will assume that  $N=4$  in all the quantitative estimates below.

here is gauged. We can imbed the conventional weak SU(2) completely in SU(2)<sub>L</sub>, and let hypercharge be generated by the  $\tau_3$  component of SU(2)<sub>R</sub>. (This imbedding is possible because the left-handed technifermion doublet has zero hypercharge.) We adopt the conventional nonlinear representation of the technipion fields:

$$\Sigma = \exp(2i\Pi/f), \quad \Sigma \rightarrow L\Sigma R^\dagger, \quad (3.2)$$

with  $\Pi$  defined in (3.1) and we write the scalar doublet  $\phi$  in matrix form:

$$\Phi = \begin{bmatrix} \bar{\phi}^0 & \phi^+ \\ -\phi^- & \phi^0 \end{bmatrix}. \quad (3.3)$$

Then, the kinetic-energy terms are given by

$$\mathcal{L}_{\text{KE}} = \frac{1}{2}\text{Tr}(D_\mu \Phi^\dagger D^\mu \Phi) + \frac{f^2}{4}\text{Tr}(D_\mu \Sigma^\dagger D^\mu \Sigma) \quad (3.4)$$

with the covariant derivative defined by

$$D^\mu \Sigma = \partial^\mu \Sigma - igW_a^\mu \frac{\tau_a}{2} \Sigma + ig'B^\mu \Sigma \frac{\tau_3}{2}. \quad (3.5)$$

Following the analysis of Ref. [4], we use the fact that  $\Phi^\dagger \Phi \propto 1$  to rewrite  $\Phi$  in terms of an isosinglet scalar field  $\sigma$ , and a unitary matrix  $\Sigma'$ :

$$\Phi = \frac{\sigma + f'}{\sqrt{2}} \Sigma', \quad (3.6)$$

where

$$\Sigma' = \exp(2i\Pi'/f'). \quad (3.7)$$

Later, we will present a more elegant redefinition of  $\Phi$  that is manifestly nonsingular in the limit  $f' \rightarrow 0$ . Since the physics is independent of the particular nonlinear field redefinition we adopt, we will work for the moment with (3.6) to derive our main results. Under this redefinition, the kinetic terms become

$$\begin{aligned} \mathcal{L}_{\text{KE}} = & \frac{1}{2}\partial_\mu \sigma \partial^\mu \sigma + \frac{f^2}{4}\text{Tr}(D_\mu \Sigma^\dagger D^\mu \Sigma) \\ & + \frac{(\sigma + f')^2}{4}\text{Tr}(D_\mu \Sigma'^\dagger D^\mu \Sigma'). \end{aligned} \quad (3.8)$$

By expanding Eq. (3.8) in terms of the component fields, it is easy to show that the pions in the linear combination

$$\pi_a = \frac{f\Pi + f'\Pi'}{\sqrt{f^2 + f'^2}} \quad (3.9)$$

become the longitudinal components of the weak gauge bosons in the unitary gauge, while those in the orthogonal linear combination,

$$\pi_p = \frac{-f'\Pi + f\Pi'}{\sqrt{f^2 + f'^2}}, \quad (3.10)$$

remain as physical scalars in the low-energy theory. In addition, we obtain the correct gauge boson masses only if

$$f^2 + f'^2 = \frac{\sin^2 \theta \cos^2 \theta}{\pi \alpha} M_Z^2 \equiv v^2. \quad (3.11)$$

From now on we will work in the unitary gauge, where the particle spectrum consists of  $\pi_p$ ,  $\sigma$ , and the massive weak gauge bosons.

Since we are interested in the determining the masses of the fields  $\pi_p$  and  $\sigma$  we need to study the scalar potential. At lowest order, it is given by

$$V_\lambda(\sigma) = \frac{\lambda}{8} [\text{Tr}(\Phi^\dagger \Phi)]^2 = \frac{\lambda}{8} (\sigma + f')^4. \quad (3.12)$$

This potential for  $\Phi$  is the only one consistent with renormalizability, gauge invariance, and our assumption that  $M_\phi = 0$ . At one loop, there are additional terms in the potential of the form  $\sigma^4 \ln(\sigma^2/\mu^2)$  induced by radiative corrections in the manner of Coleman and Weinberg [5]. These terms are important in some regions of the parameter space, however, we will begin by ignoring them. We hope that this will make the subsequent analysis easier to understand.

On the other hand, we must always include the contributions to the potential generated by the technicolor interactions. To write down all appropriate terms consistent with the chiral symmetry, we recall that the coupling of the scalar to the technifermion doublet  $\Upsilon$  is given by

$$\bar{\Upsilon}_L \begin{bmatrix} \bar{\phi}^0 & \phi^+ \\ -\phi^- & \phi^0 \end{bmatrix} \begin{bmatrix} h_+ & 0 \\ 0 & h_- \end{bmatrix} \Upsilon_R \equiv \bar{\Upsilon}_L \Phi H \Upsilon_R, \quad (3.13)$$

where  $H$  is the technifermion Yukawa coupling matrix. Thus, if we treat the matrix  $\Phi H$  as a spurion transforming as

$$(\Phi H) \rightarrow L(\Phi H)R^\dagger \quad (3.14)$$

and build all possible invariants, we will obtain the correct effective Lagrangian. In fact, we will only require the simplest term

$$\mathcal{L}_H = c_1 4\pi f^3 \text{Tr}(\Phi H \Sigma^\dagger) + \text{H.c.}, \quad (3.15)$$

where the coefficient  $c_1$  is of order unity, by naive dimensional analysis (NDA) [6]. This interaction generates a linear term in  $\sigma$ :

$$V_H(\sigma) = -\sqrt{2}c_1 4\pi f^3 (h_+ + h_-) \sigma. \quad (3.16)$$

We assume that the  $\sigma$  field has no vacuum expectation value, and therefore we require that the linear terms in  $\sigma$  vanish:

$$V'_\lambda(0) + V'_H(0) = 0 \quad (3.17)$$

or

$$\frac{\lambda}{2} f'^3 = 8\sqrt{2}c_1 \pi h f^3. \quad (3.18)$$

Together with the constraint imposed by Eq. (3.11), this completely determines the pion decay constants  $f$  and  $f'$  in terms of the model's free parameters:

$$f = v [1 + (16\sqrt{2}\pi c_1)^{2/3} (h/\lambda)^{2/3}]^{-1/2}, \quad (3.19)$$

$$f' = f (16\sqrt{2}\pi c_1)^{1/3} \left( \frac{h}{\lambda} \right)^{1/3}. \quad (3.20)$$

where  $h \equiv (h_+ + h_-)/2$ . Now it is simple to determine the scalar masses. The lowest-order contribution to  $m_\sigma^2$  comes from (3.12):

$$m_\sigma^2 = \frac{3}{2} \lambda f'^2. \quad (3.21)$$

While there are also contributions to  $m_\sigma^2$  proportional to  $f^2 h^2$ , it will be clear later that these are small corrections compared to (3.21) over the range of the parameters that will be relevant to us. For the triplet pions,  $m_\pi^2$  is generated at  $O(H)$  from the piece of (3.15) that is quadratic in  $\pi_p$ :

$$m_\pi^2 = 2c_1 \sqrt{2} \frac{4\pi f}{f'} v^2 h. \quad (3.22)$$

We will study (3.21) and (3.22) quantitatively in Sec. VI.

The reader should keep in mind that these results are not valid everywhere in the model's parameter space. Since we want perturbation theory to be reliable, we will always restrict ourselves to values of  $h$  and  $\lambda$  that are less than  $\sim 4\pi$  and  $\sim 16\pi^2$ , respectively. However, chiral perturbation theory does not give an appropriate description of the model everywhere in this region. As we increase  $h$ , the technifermion masses induced by the scalar vacuum expectation value (VEV) will eventually exceed the technicolor scale, and chiral  $SU(2) \times SU(2)$  will cease to be an approximate symmetry of the theory. Since the technifermion masses are of order  $hf'$ , the effective chiral Lagrangian is appropriate only if

$$hf' \ll 4\pi f, \quad (3.23)$$

or alternately,

$$h \ll \left[ \frac{2\sqrt{2}\pi^2}{c_1} \right]^{1/4} \lambda^{1/4}. \quad (3.24)$$

The physics of the model for  $hf' \gg 4\pi f$  would be very peculiar. The "current" masses of the technifermions produced by the breaking of the  $SU(2) \times U(1)$  would be much larger than the scale of the technicolor interactions. From an effective field theory standpoint, you might worry that the massive technifermions would not be present in the low-energy theory to produce  $SU(2) \times U(1)$  breaking. But if there were no  $SU(2) \times U(1)$  breaking, then the technifermions would be massless and then they *would* be in the low-energy theory to produce  $SU(2) \times U(1)$  breaking. As we will see in the next section, the Coleman-Weinberg interactions save us from this logical conundrum. They push us away from the region  $hf' \gg 4\pi f$  toward the region (3.24), where the chiral Lagrangian description is valid. The corrections may be important on the boundary of the allowed region. We will discuss the phenomenology of this boundary region in Sec. VIII.

Note that all of the results presented in this section could have been obtained had we chosen a different parametrization of the fields  $\Sigma$  and  $\Phi$ . For example, we could have defined

$$\Phi = \frac{1}{\sqrt{2}} \Sigma_0 (f' + \sigma + 2i\alpha\pi_p) \quad (3.25)$$

and

$$\Sigma = \Sigma_0 \exp(-2i\beta\pi_p), \quad (3.26)$$

where

$$\alpha = \frac{f}{v}, \quad \beta = \frac{f'}{fv} \quad (3.27)$$

and where

$$\Sigma_0 = \exp \left[ \frac{2i\pi_a}{v} \right] \quad (3.28)$$

with  $f^2 + f'^2 = v^2$  as before. Unlike the field redefinition given by (3.6), this choice is clearly well behaved as  $f' \rightarrow 0$ . While (3.6) appears ill defined in this limit, this is simply the consequence of a coordinate singularity. The reader can verify that either redefinition will yield the same physical results.

#### IV. COLEMAN-WEINBERG TERMS

In this section, we consider the effects of radiative corrections to the  $\sigma$  potential. The contributions will be important only when the couplings involved can grow large somewhere in our parameter space. The only Yukawa couplings that can become large are  $h_t$ , and  $h_\pm$ . Thus, to a good approximation, the corrected potential can be written

$$V(\sigma) = \frac{\lambda}{8} \sigma^4 - \frac{1}{64\pi^2} [3h_t^4 + N(h_+^4 + h_-^4)] \sigma^4 \ln \left[ \frac{\sigma^2}{\mu^2} \right] - 8\sqrt{2}\pi c_1 f^3 h \sigma, \quad (4.1)$$

where  $h_t$  is the top-quark Yukawa coupling, and  $\mu$  is an arbitrary renormalization scale. To remove the  $\mu$  dependence in (4.1), we next define the renormalized coupling  $\lambda$  conventionally as

$$\lambda \equiv \frac{1}{3} V''''(f'). \quad (4.2)$$

However, it will be convenient to describe the physics not with (4.2), but in terms of the parameter  $\tilde{\lambda}$ , defined by

$$\tilde{\lambda} \equiv \lambda + \frac{11}{24\pi^2} [3h_t^4 + N(h_+^4 + h_-^4)]. \quad (4.3)$$

We introduce the additional shift so that the condition  $V'(f') = 0$  gives us

$$f' = f (16\sqrt{2}\pi c_1)^{1/3} \left[ \frac{h}{\tilde{\lambda}} \right]^{1/3}. \quad (4.4)$$

Because of (4.4), we can take over much of the analysis of the previous section by simply making the replacement  $\lambda \rightarrow \tilde{\lambda}$ . For example, the triplet pion mass contours and condition  $hf' < 4\pi f$  look the same as before, provided we use the parameter  $\tilde{\lambda}$  instead of  $\lambda$ .

Of course, we cannot absorb all the effects of the radiative corrections into a redefinition of  $\lambda$ . The one thing that does change is the value of  $m_\sigma$ , which is determined by  $V''(f')$ . Expressed in terms of  $\tilde{\lambda}$ , we find that

$$m_\sigma^2 = \left[ \frac{3}{2} \tilde{\lambda} - \frac{1}{8\pi^2} [3h_t^4 + N(h_+^4 + h_-^4)] \right] f'^2. \quad (4.5)$$

From (4.5), it is easy to see how the theory avoids the conundrum described in the previous section. The stability of the vacuum requires  $m_\sigma^2 \geq 0$ . Thus, (4.5) implies

$$\frac{3}{2} \tilde{\lambda} \geq \frac{N}{4\pi^2} (1 + 6\delta^2 + \delta^4) h^4. \quad (4.6)$$

Together with (3.18), this implies

$$\frac{hf'}{4\pi f} \leq \left[ \frac{3c_1}{\sqrt{2}N(1 + 6\delta^2 + \delta^4)} \right]^{1/3}. \quad (4.7)$$

Thus, we never get into the dangerous region in which the effective field theory description leads us into a logical puzzle. We therefore expect that the chiral Lagrangian analysis of Sec. III will give results that are at least qualitatively correct. However, the right-hand side of (4.7) can be close to 1, so we may expect nontrivial corrections to the chiral Lagrangian relations as we approach the line  $hf' = 4\pi f$ .

## V. FLAVOR-CHANGING NEUTRAL CURRENTS

In this section, we set up the analysis of flavor-changing neutral currents in our model. The coupling of the scalar doublet  $\phi$  to the ordinary quarks can be written in matrix form:

$$\bar{\psi}_L \Phi \begin{pmatrix} h_U & 0 \\ 0 & V h_D \end{pmatrix} \psi_R + \text{H.c.}, \quad (5.1)$$

where  $\psi_L = (U_L, VD_L)$ ,  $\psi_R = (U_R, D_R)$ ,  $h_U = \text{diag}(h_u, h_c, h_t)$ ,  $h_D = \text{diag}(h_d, h_s, h_b)$ , and where  $V$  is the CKM matrix. After applying (3.6), these couplings become

$$\frac{\sigma + f'}{\sqrt{2}} \bar{\psi}_L \Sigma' \begin{pmatrix} h_U & 0 \\ 0 & V h_D \end{pmatrix} \psi_R + \text{H.c.} \quad (5.2)$$

from which we extract the charged-pion couplings

$$i \left[ \frac{f}{v} \right] [\bar{D}_L V^\dagger \pi_p^- h_U U_R + \bar{U}_L \pi_p^+ V h_D D_R + \text{H.c.}] \quad (5.3)$$

The physical pions contribute to the  $\Delta q = 2$  box diagrams shown in Fig. 1, where<sup>2</sup>  $q = S$  or  $B$ . Notice that the explicit factors of the top-quark Yukawa coupling in these diagrams cause the two-top-quark exchange diagrams to dominate over all others. For the two-pion exchange diagram, we find that the contribution to the operator  $\{\bar{q} \gamma^\mu [(1 + \gamma_5)/2] d\}^2$  is given by

$$2 \left[ \frac{f}{f'v} \right]^4 m_t^4 (V_{td} V_{tq}^*)^2 I_1(m_t, m_\pi), \quad (5.4)$$

<sup>2</sup>We omit a discussion of  $D^0 - \bar{D}^0$  mixing, because we found this process to provide much weaker constraints on the model.

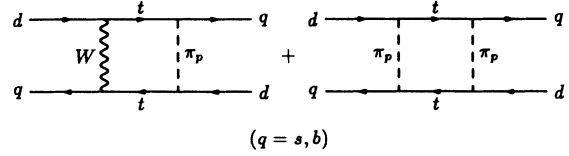


FIG. 1. Nonstandard box diagrams for one- and two-pion exchange.

while the one-pion- $W$  exchange diagram gives us

$$g^2 \left[ \frac{f}{f'v} \right]^2 m_t^4 (V_{td} V_{tq}^*)^2 \left[ I_2(m_t, m_\pi) + \frac{1}{4m_W^2} I_3(m_t, m_\pi) \right]. \quad (5.5)$$

Similar box diagrams are generated in two-Higgs doublet models, and the integrals  $I_j$  ( $j=1, \dots, 3$ ) have been tabulated previously [7]. We provide them in the Appendix. In evaluating these diagrams, we have neglected the four-momenta of all external particles; this is a good approximation because the masses of the  $s$  and  $b$  quarks are small compared to the masses of the particles running around the loop. For comparison, we note that the standard contribution to the coefficient of  $\{\bar{q} \gamma^\mu [(1 + \gamma_5)/2] d\}^2$  is of the order

$$\frac{G_F^2}{4\pi^2} m_c^2 (V_{cd} V_{cs}^*)^2 \quad (5.6)$$

for  $K^0 - \bar{K}^0$  mixing, and

$$\frac{G_F^2}{4\pi^2} m_t^2 (V_{td} V_{tb}^*)^2 \quad (5.7)$$

for  $B^0 - \bar{B}^0$  mixing. We will analyze these results quantitatively in the following section.

## VI. EXPERIMENTAL LIMITS

We are now prepared to compare the predictions of our model to experiment. As discussed in Sec. II, we will strive to systematically exclude regions of the  $\lambda$ - $h$  plane. We immediately truncate our plots at  $h = 4\pi$  and  $\lambda = 16\pi^2$ , and we show the  $hf' = 4\pi f$  line to indicate where there may be sizable corrections to the chiral Lagrangian analysis.

Our first concern is that the scalar states in our model must be heavy enough to avoid detection. The ALEPH Collaboration [8] has placed the strongest lower limit on the mass of a neutral Higgs boson by studying the process  $Z \rightarrow Z^* H$ , assuming the standard model coupling

$$\frac{ve^2}{4s^2 c^2} Z^\mu Z_\mu H. \quad (6.1)$$

They exclude a mass less than 48 GeV at the 95% confidence level. We display the  $m_\sigma = 48$  GeV contour in Fig. 2. The allowed region is inside the solid curve. As discussed in the previous section, because of the Coleman-Weinberg terms in the potential,  $m_\sigma$  depends on  $m_t$  and  $\delta$ . The solid line in Fig. 2 corresponds to

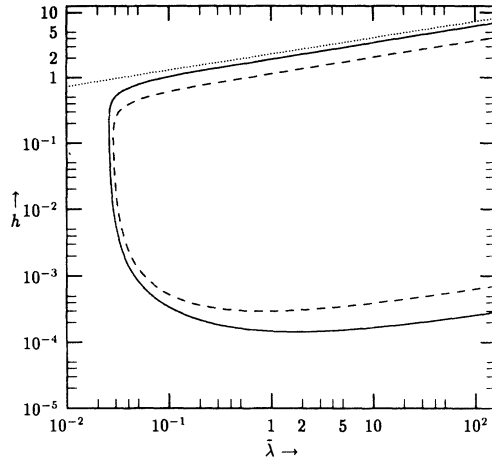


FIG. 2. The  $m_\sigma=48$  GeV line. The solid line is  $m_t=110$  GeV,  $\delta=0$ . The dashed line is  $m_t=150$  GeV,  $\delta=1$ . The dotted line is  $hf'=4\pi f$ .

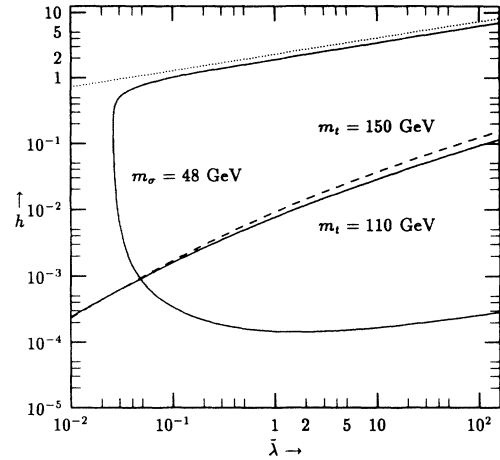


FIG. 4. Parameter space excluded by  $B^0\text{-}\bar{B}^0$  mixing; the region above the  $B$  line and to the right of the 48-GeV contour is allowed.

$m_t=110$  GeV and  $\delta=0$ . The Yukawa coupling,  $h_t$ , gets large as  $h$  gets small [see (3.20)], thus the effect of  $m_t$  is large near the bottom of the  $m_\sigma$  curve. Larger values of  $m_t$  move the bottom of the curve upwards. The effect of the technifermion Yukawa couplings is large for large  $h$ , and thus the  $\delta$  dependence is largest at the top of the curve. Increasing  $\delta$  moves the top of the curve down. The dashed line corresponds to  $m_t=150$  GeV and  $\delta=0$ .

It is important to keep in mind that the  $ZZ\sigma$  coupling in our model is given by

$$\frac{f'e^2}{4s^2c^2} Z^\mu Z_\mu \sigma \tag{6.2}$$

and hence the  $\sigma$  production rate is suppressed compared to the standard model by a factor of  $(f'/v)^2$ . Thus, the

48-GeV contour is not equivalent to the CERN  $e^+e^-$  collider LEP limit everywhere. However, we will see shortly out that in the region of parameter space not excluded by flavor-changing neutral currents,  $f'/v \sim 1$  along the  $m_\sigma=48$  GeV line, and it therefore serves as an approximate boundary to the experimentally allowed region.

In Figs. 3 and 4, we show a rough estimate of the flavor-changing neutral current limits, generated by requiring that the sum of the nonstandard box diagrams, (5.4) and (5.5), not exceed the standard model estimates given in (5.6) and (5.7). We show the results for two representative values of the top-quark mass,  $m_t=110$  and 150 GeV. Evidently, as the experimental lower bound on  $m_t$  increases, the flavor-changing neutral current limits tighten. The region in parameter space excluded by  $K^0\text{-}\bar{K}^0$  and  $B^0\text{-}\bar{B}^0$  mixing lies below the “ $K$  line” and “ $B$

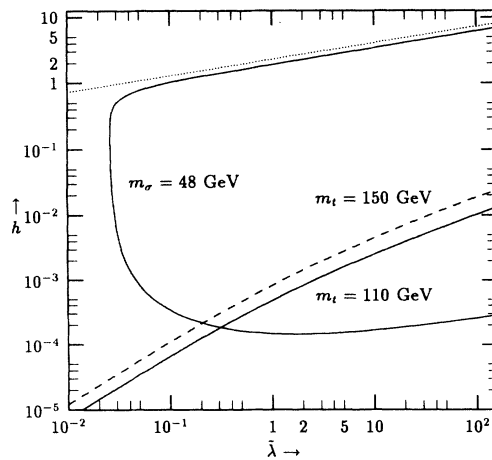


FIG. 3. Parameter space excluded by  $K^0\text{-}\bar{K}^0$  mixing; the region above the  $K$  line and to the right of the 48-GeV contour is allowed.

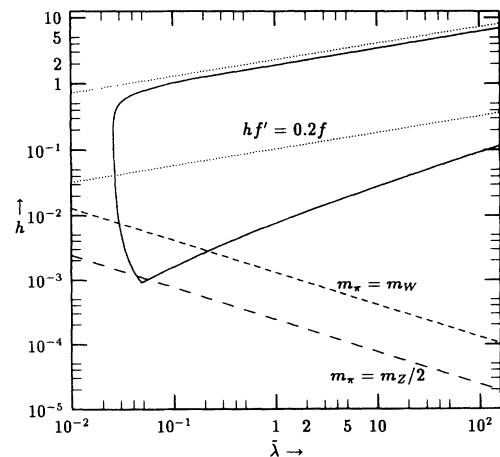


FIG. 5. Parameter space showing the  $m_\pi=m_Z/2$ ,  $m_\pi=m_W$ , and  $hf'=0.2f$  lines.

line," respectively. We see that  $B^0\text{-}\overline{B}^0$  mixing provides the more stringent limits, but by no means exclude all of the available parameter space. Everything above the  $B$  line, and to the right of the  $m_\sigma=48$  GeV contour, is allowed, and much of this parameter space is within the region in which our chiral expansion is trustworthy.

We must also consider the possibility of detecting the isotriplet pions  $\pi_p$ . In Fig. 5, we show the contour of the allowed region from Fig. 4 (with  $m_t=110$  GeV), with the  $m_\pi=m_Z/2$  and  $m_\pi=m_W$  lines as points of reference. For all of the parameter space above the  $B$  line,  $m_\pi > m_Z/2$  so that the decay  $Z \rightarrow 2\pi_p$  is not kinematically allowed. In particular, we obtain little useful information from the available LEP limits on  $Z \rightarrow \pi_p^+ \pi_p^-$ . In fact, for most of the parameter space,  $m_\pi$  is larger than  $m_Z$ , and the triplet pions cannot be produced in any weak gauge boson decays.

## VII. OBLIQUE CORRECTIONS

For completeness, we now will consider the effect of the nonstandard scalars in our model on oblique electroweak radiative corrections. In particular, we will estimate the  $S$  and  $T$  parameters, which have been shown to provide stringent constraints on simple technicolor models [9]. The low-energy contributions to these parameters can be computed within the framework of our effective chiral Lagrangian by evaluating pion loop diagrams. The results for  $S$  will depend only on our location in the  $\lambda$ - $h$  plane, and on the unknown coefficients in the chiral Lagrangian. To compute  $T$ , however, we will also need to specify the parameter  $\delta$ , which determines the magnitude of custodial isospin violation in the technicolor sector. Since we do not know the value of  $\delta$ , the sign of the nonstandard contribution, or size of the top-bottom mass splitting, our ability to constrain the model is somewhat diminished. What we will show is that the new contributions to  $T$  are not dangerously large in much of the parameter space, assuming the worst case scenario in which  $\delta=1$ . Thus, we will demonstrate that  $h_+$  and  $h_-$  do not require fine-tuning in this model. Note that we have separated the discussion of oblique corrections from Sec. VI because we will be unable to exclude any additional region of the  $\lambda$ - $h$  plane.

The  $S$  parameter can be expressed as

$$S = -16\pi \left[ \frac{d}{dq^2} \Pi_{3B} \right]_{q^2=0}, \quad (7.1)$$

where  $\Pi_{3B}$  is the piece of  $W_3 B$  vacuum polarization proportional to  $ig^{\mu\nu}$ . There is a tree-level contribution to  $S$  from the following term in the chiral expansion:

$$\frac{c_2}{16\pi^2} \text{Tr}(\Sigma^\dagger W^{\mu\nu} \Sigma B_{\mu\nu}), \quad (7.2)$$

where  $W^{\mu\nu}$  and  $B^{\mu\nu}$  are the gauge field strength tensors, and where  $c_2$  is a constant of order unity. The contribution to  $S$  is then given by

$$S_0 = \frac{1}{\pi} c_2. \quad (7.3)$$

$S_0$  originates from the nonperturbative, high-energy dynamics, and hence is proportional to an undetermined parameter in the low-energy theory. This high-energy technicolor contribution to  $S$  has been estimated in Ref. [9], and is given by<sup>3</sup>

$$S_0 \approx 0.3 \frac{N_{\text{TF}}}{2} \frac{N}{3} = 0.1N \quad (7.4)$$

for a model with two techniflavors. In this estimate,  $S$  is normalized so that  $S=0$  corresponds to the standard model with a 1-TeV Higgs boson. We adopt this convention throughout. Assuming that  $S$  is positive, then the experimental upper bound is given by [10]

$$S < 0.9 \quad (7.5)$$

at the 95% confidence level. We need to verify that the low-energy contributions in our model do not exceed the difference between (7.5) and (7.4), for an appropriate choice of  $N$ .

The low-energy contributions to  $\Pi_{3B}$  in our model are obtained from the one-loop vacuum polarization diagrams shown in Figs. 6(a)–6(c). Working in the modified minimal subtraction (MS) prescription, we find

$$\Delta S_a = \frac{1}{12\pi} \ln \left[ \frac{\mu^2}{m_\pi^2} \right], \quad (7.6)$$

$$\Delta S_b = -\frac{1}{12\pi} \frac{f^2}{v^2} \left[ \ln \left[ \frac{\mu^2}{m_\pi^2} \right] - 2(x+x^2) + (3x^2+2x^3) \ln \left[ 1 + \frac{1}{x} \right] + \frac{5}{6} \right], \quad (7.7)$$

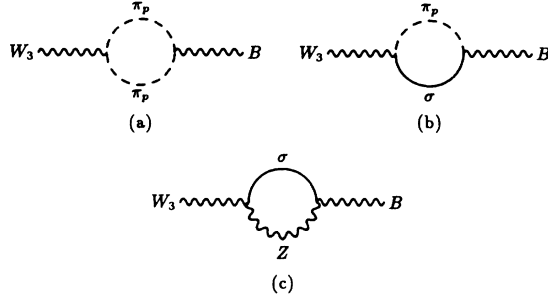
$$\Delta S_c = -\frac{1}{12\pi} \frac{f'^2}{v^2} \left[ \ln \left[ \frac{\mu^2}{m_\sigma^2} \right] + (4y+10y^2) - (9y^2+10y^3) \ln \left[ 1 + \frac{1}{y} \right] + \frac{5}{6} \right], \quad (7.8)$$

where  $x \equiv m_\sigma^2/(m_\pi^2 - m_\sigma^2)$  and  $y \equiv m_Z^2/(m_\sigma^2 - m_Z^2)$ . Note that the sum of the three diagrams that we consider here is finite, and therefore the sum of (7.6)–(7.8) is independent of the cutoff  $\mu$ . Since a reference value of  $S$  has already been subtracted in the definition of  $S_0$ , as we pointed out earlier, our final estimate of the low-energy contribution is given by

$$\Delta S = \Delta S_a + \Delta S_b + \Delta S_c. \quad (7.9)$$

To get some idea of the characteristic size of  $\Delta S$ , we evaluate it along the  $h=0.2f/f'$  line shown in Fig. 5.

<sup>3</sup>In Ref. [4] this estimate was multiplied by an extra factor of  $v^2/f^2$ ; we now believe this is an error. Without this factor, the value of  $S_0$  in Ref. [4] is reduced and the conclusion that the massive scalar model is viable is strengthened.

FIG. 6. Vacuum polarization diagrams contributing to  $\Pi_{3B}$ .

This line was chosen because it is in the heart of the allowed region, and well within the area where our chiral Lagrangian is valid. Along this path, the value of  $\Delta S$  is plotted in Fig. 7. We see that  $\Delta S$  ranges from roughly  $-0.11$  to  $0.01$ ; in any event, it is not very large. For a reasonable choice of  $N$ , e.g.,  $N=4$ , the high-energy contribution is  $0.4$ , and dominates over the low-energy component. The total contribution in this particular example then ranges from  $0.29$  to  $0.41$ , which is consistent with the experimental bounds.

The  $T$  parameter is defined in terms of a different combination of vacuum polarizations

$$T = \frac{4\pi}{s^2 c^2 m_Z^2} [\Pi_{11} - \Pi_{33}]_{q^2=0}. \quad (7.10)$$

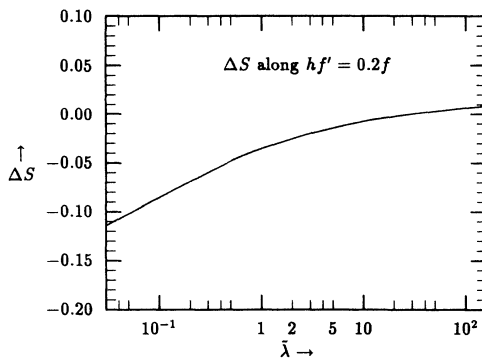
To estimate  $T$ , we again start by considering the tree-level contributions to  $\Pi_{11} - \Pi_{33}$ , which come from terms in our chiral expansion of the form

$$\mathcal{L} = \frac{c_3}{16\pi^2} (\text{Tr} \Phi H D^\mu \Sigma^\dagger)^2. \quad (7.11)$$

From (7.11) we obtain a result of order

$$\Delta T = \frac{1}{8\pi^2 \alpha} \left( \frac{f'}{v} \right)^2 h^2 \delta^2, \quad (7.12)$$

which is relatively small throughout much of the allowed region. However, (7.12) does not represent the leading

FIG. 7. Low-energy contribution to  $S$ .

contribution. The one-loop diagrams that incorporate the mass splitting of the pion triplet give us contributions to  $T$  that are logarithmically enhanced over (7.12). The pion masses are split at  $O(H^2)$  by the effects of the term

$$c_4 f^2 \text{Tr}(\Phi H \Sigma^\dagger \Phi H \Sigma^\dagger) + \text{H. c.} \quad (7.13)$$

From (7.13) we find

$$m_{\pi_0}^2 - m_{\pi^\pm}^2 = 4c_4 v^2 h^2 \delta^2. \quad (7.14)$$

We may now compute the one-loop diagrams shown in Fig. 8 by working to lowest order in  $m_{\pi_0}^2 - m_{\pi^\pm}^2$ , and substituting (7.14). We obtain

$$\Delta T = \frac{4c_4}{\alpha} h^2 \delta^2 \left[ \left( \frac{f}{v} \right)^2 F(m_\sigma, m_{\pi_0}) + F(m_{\pi^\pm}, m_{\pi_0}) \right], \quad (7.15)$$

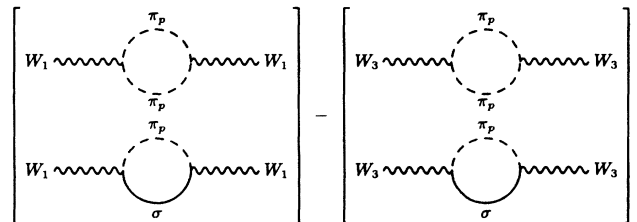
where

$$F(m_1, m_2) = \frac{1}{16\pi^2} \left[ \ln \left( \frac{\mu^2}{m_2^2} \right) + \frac{m_1^4}{(m_1^2 - m_2^2)^2} \ln \left( \frac{m_2^2}{m_1^2} \right) + \frac{m_1^2}{(m_1^2 - m_2^2)} \right] \quad (7.16)$$

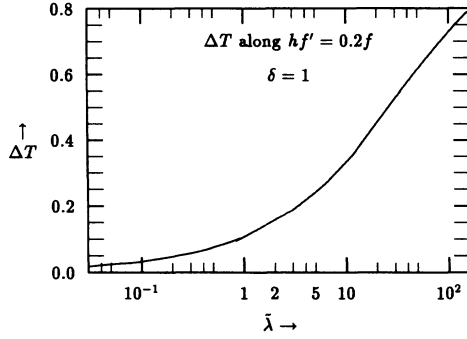
and where we set  $\mu$  equal to the technicolor scale,  $4\pi f$ . In fact, only the logarithmically enhanced term is of any real interest to us in this result. The  $1/\epsilon$  poles in the loop integrals have been removed by introducing counterterms of the form (7.11). However, as we have seen, these terms also contribute an unknown finite amount to  $\Delta T$ . The point of our computation is that the logarithmic term is large enough so that we do not need to worry about all the unknown finite contributions in order to obtain a reliable estimate.

Again we evaluate our results along the  $h=0.2f/f'$  line shown in Fig. 5, setting  $\delta=1$ . The results are plotted in Fig. 9.

We see that these results present no imminent danger of conflict with the experimental bounds on  $T$ , at least in most of the region of the parameter space that we have sampled. In fact, we could adjust  $\delta$  from  $1$  to  $\frac{1}{5}$  and suppress the results shown by a factor of  $\frac{1}{5}$ , without introducing any substantial fine-tuning. Since  $\Delta T$  is proportional to  $h^2$ , it seems that the necessity of fine-tuning  $\delta$  may arise at larger values of  $h$ , but this is exactly the

FIG. 8. Vacuum polarization diagrams contributing to  $\Pi_{11} - \Pi_{33}$ .



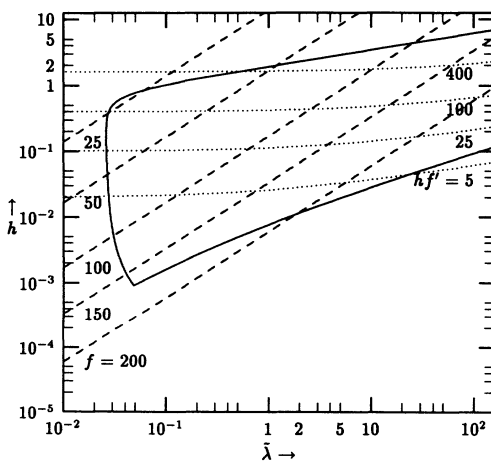
FIG. 9. Low-energy contribution to  $T$ .

limit in which our chiral expansion begins to break down. We will therefore need to reexamine this question in next section.

### VIII. BEYOND THE CHIRAL EXPANSION

At the bottom of the allowed region in Fig. 5, our model looks like a rather standard technicolor model, like that discussed in [4]. However, near the top of the allowed region, the physics is very different. A full discussion of the phenomenology of this region is beyond the scope of this paper, but we would like at least to explain what is so peculiar about it. The essential point is illustrated in Fig. 10, where we have plotted contours of fixed  $f$  (the dashed lines) and  $hf'$  (the dotted lines).

At the top of the allowed region, the technicolor scale,  $f$ , can be considerably smaller than the average “current” mass of the technifermions  $h_{\pm}f'$ . While the ratio  $hf'/f$  cannot grow arbitrarily large because of the Coleman-Weinberg corrections discussed in Sec. IV, the ratio does get close to  $4\pi$ , and that is enough to drastically change the physics of the technifermion bound states. The technifermions in this region are much more analogous to  $c$  quarks in QCD than they are to  $u$  and  $d$  quarks. In par-

FIG. 10. Values of  $f$  and  $hf'$ .

ticular, one might expect that the vector bound states of these technifermions will be quite narrow, like the  $J/\psi$ .

Note also that  $hf'$  is the average current mass of the technifermions. If  $\delta$  is very different from zero, one of technifermion masses will be smaller. This is quite interesting in the upper left-hand corner of the allowed region, where the technicolor scale is quite small. Here one can imagine that some of the technifermions bound states might even be light enough to show up at LEP II energies. The lightest state will presumably be a bound state of the lighter technifermions, and therefore it will be neutral and can be produced at LEP II if it is light enough. On the other hand, this may make a large contribution to the  $T$  parameter through mixing of the lightest state with the  $Z$ .

### IX. CONCLUSIONS

We have presented a minimal technicolor model, in which the ordinary fermions and technifermions are coupled by a massless scalar doublet. The technicolor condensate that breaks the electroweak symmetry also drives the scalar's vacuum expectation value, which, in turn, generates the fermion masses. Flavor symmetry breaking originates from Yukawa couplings, as in the standard model. We have shown that the scalar states in the theory can be made massive enough to avoid detection, even though the high-energy theory has no mass terms, and no arbitrary dimensionful parameters. In addition, we have shown that the model does not generate unacceptably large flavor-changing neutral currents, nor does it give a large low-energy contribution to the  $S$  or  $T$  parameter.

Our model is nearly as parsimonious as the standard model with a single fundamental scalar doublet. There are only two more continuous parameters  $h_{\pm}$ . The technicolor scale  $\Lambda_{TC}$  plays the role in our model that the scalar mass term plays in the simplest standard model—it sets the mass scale for all light particle states. In terms of parameter counting, *our model is the simplest extension of the standard model*. The next simplest, the two-doublet model, even with the scalar masses set to zero, has one more renormalized parameter than ours.

While in the final analysis we cannot argue that a model with a fundamental massless scalar at the electroweak scale is natural, we have nonetheless demonstrated that our model is both simple and consistent with the current experimental constraints. In contrast, the fully massless, Coleman-Weinberg limit of the standard model produces a Higgs boson that is unacceptably light after symmetry breaking. Technicolor helps us by making the physical scalar states in our model heavy enough to avoid detection. In the end, we are left with a fully massless theory that is viable, and has a rich and interesting phenomenology.

### ACKNOWLEDGMENTS

This work was supported in part by the National Science Foundation, under Grant No. PHY-9218167, and in part by the Texas National Research Laboratory Commission under Grant No. RGFY93-278B.

## APPENDIX

Below are the integrals relevant to the box diagram calculations in Sec. V. They are in agreement with those published previously in Ref. [7]:

$$I_1(m_1, m_2) = \int_E \frac{d^4 k}{(2\pi)^4} \left[ \frac{k^2}{(k^2 + m_1^2)(k^2 + m_2^2)} \right]$$

$$= \frac{1}{16\pi^2} \left[ \frac{m_2^2 + m_1^2}{(m_2^2 - m_1^2)^2} + \frac{2m_1^2 m_2^2}{(m_2^2 - m_1^2)^3} \ln \left[ \frac{m_1^2}{m_2^2} \right] \right], \quad (\text{A1})$$

$$I_2(m_1, m_2) = \int_E \frac{d^4 k}{(2\pi)^4} \left[ \frac{1}{(k^2 + m_1^2)^2 (k^2 + m_2^2) (k^2 + M_W^2)} \right]$$

$$= \frac{1}{16\pi^2} \left[ \frac{m_2^2 \ln(m_1^2/m_2^2)}{(m_2^2 - m_1^2)^2 (m_2^2 - M_W^2)} + \frac{M_W^2 \ln(m_1^2/M_W^2)}{(M_W^2 - m_1^2)^2 (M_W^2 - m_2^2)} - \frac{1}{(m_1^2 - m_2^2)(m_1^2 - M_W^2)} \right], \quad (\text{A2})$$

$$I_3(m_1, m_2) = \int_E \frac{d^4 k}{(2\pi)^4} \left[ \frac{k^2}{(k^2 + m_1^2)^2 (k^2 + m_2^2) (k^2 + M_W^2)} \right]$$

$$= \frac{1}{16\pi^2} \left[ \frac{m_2^4 \ln(m_2^2/m_1^2)}{(m_2^2 - M_W^2)(m_1^2 - m_2^2)^2} + \frac{M_W^4 \ln(M_W^2/m_1^2)}{(M_W^2 - m_2^2)(m_1^2 - M_W^2)^2} + \frac{m_1^2}{(m_1^2 - m_2^2)(m_1^2 - M_W^2)} \right]. \quad (\text{A3})$$

- 
- [1] S. Dimopoulos and L. Susskind, Nucl. Phys. **B155**, 237 (1977); E. Eichten and K. Lane, Phys. Lett. **90B**, 125 (1980).
- [2] R. S. Chivukula and H. Georgi, Phys. Lett. B **188**, 99 (1987); S. Dimopoulos, H. Georgi, and S. Raby, *ibid.* **127B**, 101 (1983); R. S. Chivukula, H. Georgi, and L. Randall, Nucl. Phys. **B292**, 93 (1987).
- [3] E. H. Simmons, Nucl. Phys. **B312**, 253 (1989); S. Samuel, *ibid.* **B347**, 625 (1990); A. Kagan and S. Samuel, Phys. Lett. B **252**, 605 (1990); **270**, 37 (1991).
- [4] C. D. Carone and E. H. Simmons, Nucl. Phys. **B397**, 591 (1993).
- [5] S. Coleman and E. Weinberg, Phys. Rev. D **7**, 1888 (1973).
- [6] S. Weinberg, Physica A **96**, 237 (1979); A. Manohar and H. Georgi, Nucl. Phys. **B234**, 189 (1984); L. Randall, *ibid.* **B 276**, 241 (1986); T. Applequist, in *Gauge Theories and Experiments at High Energies*, Proceedings of the 21st Scottish Universities Summer School in Physics, St. Andrews, Scotland, 1980, edited by K. C. Bowler and D. G. Sutherland (SUSSP, Edinburgh, 1981), p. 385.
- [7] L. F. Abbott, P. Sikivie, and M. B. Wise, Phys. Rev. D **21**, 1393 (1980).
- [8] D. Decamp *et al.*, Phys. Rep. **216**, 253 (1992).
- [9] M. E. Peskin and T. Takeuchi, Phys. Rev. Lett. **65**, 964 (1990); Phys. Rev. D **46**, 381 (1992).
- [10] T. Takeuchi, in *Proceedings of the International Workshop on Electroweak Symmetry Breaking*, Hiroshima, 1991, edited by W. A. Bardeen, J. Kodaira, and T. Muta (World Scientific, Singapore, 1992).